ORIGINAL ARTICLE

Replacing IR Wavelength Instead of Visible Wavelength on the BG Network Model to Improve the Effects of Optogenetic Stimulation in Parkinson's Disease

Shabnam Andalibi Miandoab [1, 2*], **Nazlar Ghasemzadeh** [3*]

Department of Electrical Engineering, Tabriz Branch, Islamic Azad University, Tabriz, Iran

Biophotonic Research Center, Tabriz Branch, Islamic Azad University, Tabriz, Iran

Department of Biomedical Engineering, Tabriz Branch, Islamic Azad University, Tabriz, Iran

*Corresponding Authors: Shabnam Andalibi Miandoab, Nazlar Ghasemzadeh
Email: sh.andalibi@iaut.ac.ir, n.ghassemzadeh@iaut.ac.ir

Received: 08 October 2024 / Accepted: 26 November 2024

Abstract

Purpose: In optogenetics, visible light is usually used, which limits the penetration depth into the tissue, and placing optical fibers to deliver light to deep areas of the brain is necessary. In this paper, to overcome limitations, the use of Near-Infrared light (NRI) and temperature-sensitive opsins has been proposed as a powerful, non-invasive, or minimally invasive tool due to greater penetration depth, with the least damage and most effectiveness in brain tissue.

Materials and Methods: Effects of optogenetic stimulation with visible light and NIR on the model of Parkinson's Disease (PD) Basal Ganglia-Thalamic (BG-Th) network to reduce or eliminate pathological effects of Parkinson's disease has been studied. Three and four-state optogenetic Halordopsin (NpHR) and Channelrhodopsin-2 (ChR2) opsins at visible wavelengths and four-state optogenetic with Transient Receptor Potential Vanilloid 1 (TRPV1) and Transient Receptor Potential Ankyrin 1 (TRPA1) opsins at NIR wavelengths for different frequencies and number of stimulation pulses and light intensity on Error Index (EI) and beta band activity in the BG-TH to introduce optimal values for basic parameters of f, ns, and Alight have been considered. Finally, we obtained Alight effects on the beta band activity for different optogenetic stimulations and opsins (NpHR, ChR2, TRPV1, and TRPA1).

Results: Four-state optogenetic stimulation TRPA1 at 808 nm is optimal with the best results, lowest EI, and beta band activity. By increasing Alight, beta band activity for all used opsins has decreased, which is sharp for NpHR, and TRPA1 with 808 nm, with low intensity, has caused less beta band activity.

Conclusion: The Near-Infrared light with the best results and the lowest beta band activity (Beta activity=0.2) is more effective.

Keywords: Parkinson's Disease; Optogenetic; Infrared Neural Stimulation; Basal Ganglia Network Model.

DOI: https://doi.org/10.18502/fbt.v12i2.18278

Frontiers in BIOMEDICAL TECHNOLOGIES

1. Introduction

Parkinson's Disease (PD) is the second neurodegenerative disorder after Alzheimer's disease (AD), and it has affected a large part of the elderly population [1, 2]. According to statistics, 7 million to 10 million people in the world are struggling with Parkinson's disease [3]. Parkinson's disease is a movement disorder characterized by the neurodegeneration of the dopamine neurons of the basal ganglia (BG) of the brain in the substantia nigra pars compacta (SNc) and Ventral Tegmental Area (VTA) [4]. BG is a subcortical brain structure that plays an important role in the movement system and regulates movement by using a certain amount of dopamine. Excessive dopamine can lead to involuntary and spontaneous activities, while its deficiency leads to blunt incoordination and slow movement reactions [5]. PD leads to vigorous and long-lasting oscillation of the beta band in the BG of the brain. The main symptoms of PD are tremors, muscle rigidity, akinesia, and dysphonia [6]. Functional and structural studies of ion channels have deepened our understanding of their mechanism and essential role in regulating neuronal activity and treating diseases. Conventional methods of treating diseases have limitations such as invasiveness, irreversibility, and low spatial and temporal resolution, which limit their clinical application. Therefore, using non-invasive or minimally invasive ion channels (opsin/gene) is desirable. Ion channels form the molecular basis of bioelectricity, and by creating resting membrane potentials, they balance electrostatic charges and maintain ion homeostasis in the cell membrane. Dysfunction of ion channels is associated with neurodegenerative diseases such as Parkinson's disease, cardiovascular disease, kidney and lung diseases [7-11].

Optogenetics uses light to stimulate genetically altered neurons by modulating the channels. It has revolutionized neuroscience due to its outstanding advantages, such as spatial and temporal resolution, ability to control light on-off, cell-type specificity, and low toxicity [12, 13].

In optogenetics, the application of light is usually in the range of the visible light spectrum, which limits the depth of tissue penetration, so surgical placement of optical fibers is required to deliver light to deep areas, which in turn leads to infection and irreversible damage to the tissue and it is an invasive method [7]. Optogenetics combines genetic and optical engineering methods to precisely control biological events in specific neurons in real-time. It uses light-sensitive ion channels or pumps to inhibit or activate physiological processes under illumination at a particular wavelength. In general, the ChR channels are the most common rhodopsins used more often, depolarizing the neurons and creating action potentials [14]. Halorodopsins (NpHRs) are chloride-type ion pumps that allow chlorine ions to enter neurons and lead to the inhibition and suppression of neuronal activity [7]. Despite the revolutionary role of optogenetic, the wavelength of used opsins in the range of visible light, which, as previously mentioned, has a series of problems, including low penetration depth into the tissue, the need for optical fiber implantation, causing tissue damage, inflammation, and infection, and finally creating movement artifacts and unstable signals due to the frequent movement of the fiber. Therefore, to overcome these limitations, Near-Infrared (NIR) light is recommended [7]. NIR, which is in the range of 780-1100nm, has been widely used as a powerful non-invasive or minimally invasive tool due to its greater penetration depth, less absorption, and less scattering by inducing minimal tissue damage, with the greatest effectiveness in medical research for the diagnosis and treatment of neurological diseases, especially in the brain [15-20].

Since the use of NIR light, to some extent, creates local heat in the tissue, opsins that are sensitive to temperature and active with NIR light are required. Temperature-sensitive ion channels are composed of several separate proteins necessary to maintain thermal homeostasis in the body. Transient Receptor Potential (TRP) cation channels are one of the most well-known temperature-sensitive ion channels, which have different types, including Transient Receptor Potential Vanilloid 1-4(TRPV1-V4), Transient Receptor Potential Melastatin 8 (TRPM8), and Transient Receptor Potential Ankyrin 1 (TRPA1) [7, 21, 22]. Pui-Ying Lam *et al.* (2020) [23] have introduced a variety of effective temperature-sensitive opsins with high conductivity in optogenetics to activate neurons using NIR. Yuxia Liu *et al.* (2022) [7] investigated the manipulation and use of different ion channels as therapeutic methods in neurological diseases on animal models using optogenetic and NIR

as a non-invasive or minimally invasive method. Wei–Hsu Chen *et al.* (2022) [21] have studied and investigated the use of TRPV1 temperature-sensitive opsins in optogenetics for neurons using NIR in a non-invasive manner. In this paper, since visible light can limit the penetration depth into the brain tissue, reaching the depth areas of the brain tissue requires the placement of optical fibers, which is invasive, so we have used the NIR light with thermally sensitive opsins. NIR light has great penetration depth, which can be a strong, non-invasive, or minimally invasive tool along with temperature-sensitive opsins without thermal effect and the least damage to brain tissue. We have considered the complete computational BG-Th network model based on the Terman *et al.* model. Our proposed model consists of all the brain parts affected by PD (Thalamus (TH), Globus Pallidus internus (GPi), Globus Pallidus externus (GPe), and Subthalamic nucleus (STN)). The BG-Th network model has been represented in Figure 1a, b, with TH, GPi, GPe, and STN neurons and sparse connections between STN, GPe, GPi, and TH cells. The Sensorimotor Cortex (SMC) input has been inserted into the Th cells. The I_appcurrent has been applied to each of the STN, GPe, and GPi cells. The cells of the BG-Th model network have been modeled as conductance-based in the Hodgkin–Huxley system of the differential equations. Four and three- state optogenetic stimulations with the light and thermal sensitive opsins of the ChR2, NpHR, TRPV1, and TRPA1 which are activated by visible and NIR light (480 nm, 570 nm, 808 nm, and 980 nm), have been inserted to the GPi, GPe, and STN neuron. Furthermore, we have developed a complete computational model to obtain the effective ranges of three and four state optogenetic stimulation with different opsins for NIR and visible wavelengths in PD on error index (EI) and BG beta activity. We have presented changing the basic parameters (frequency (f), number of stimulation pulses (ns), light intensity (Alight) and introduced the optimal parameters. The advantage of the computational model is that without the need for living tissue, the appropriate values of frequency, number of stimulation pulses, wavelength, and light intensity can be obtained with minimal damage. The EI is a quantitative measure of thalamic function as described by Rubin and Treman (2004) [24]. Thus, the performance of the BG network model is evaluated by measuring how correctly TH neurons respond to SMC inputs [25]. Also, we have analyzed the EI and Beta activities for the SMC inputs, a series of monophasic current pulses with an amplitude of $0.035 pA/\mu m^2$ with pulse width of 5ms during our simulation. Beta-band activity in PD is the synchronous and oscillatory neuronal activity of BG network model neurons. In PD, the beta band activity of BG network model neurons is high due to the death of dopamine-producing neurons in the BG of the brain, which leads to an increase in the strength of synaptic connections (gsyn) of BG neurons and a decrease in input from different parts of the brain such as the striatum to BG neurons. (Iapp) that manage the inhibition and excitability of BG neurons. Therefore, the increase of Iapp and the decrease of gsyn can decrease the activity of the beta band [26]. Consequently, it is very important to investigate the effects of beta activity in our proposed model. According to recent reports, damage to the superficial cortical tissue occurs at A>100mw/mm^2. However, light intensity A<75mw/mm^2 is sufficient to induce neural activity [27]. When the intensity of light stimulation is high enough, due to the conversion of a large part of the energy into heat, it can cause thermal damage in the tissue [28]. Therefore, it is very important to achieve a better therapeutic effect at low levels of light stimulation intensity. To achieve these goals, we performed three-state optogenetic with NpHR opsin (with visible light of 570 nm) and four-state optogenetic with opsin ChR2 (with visible light of 480 nm), three- and four-state optogenetic of TRPV1 and TRPA1 with NIR light (808 and 980 nm).

To compare and investigate the effects of these stimulations, we have considered EI and beta band activity by changing the intensity of light stimulation (Alight) in the BG network model for frequencies (f=20-220 Hz) and number of stimulation pulses (ns=10 -60). Based on the results, the optimal stimulation model is the four-state optogenetic stimulation with opsin TRPA1 with a wavelength of 808 nm with the best results and the lowest range for EI (0 to 0.35) and beta band activity (0 to 3.5). On the other hand, the results of four-state optogenetic stimulation with ChR2 opsin are more consistent with the results of existing valid experiments (two groups of monkeys). Finally, by changing the intensity of light stimulation (Alight), we have obtained its effects on the activity of the beta band for different optogenetic stimulations for different opsins. Based on

that, with the increase of Alight, the activity of the beta band for all opsins (NpHR, ChR2, TRPV1, and TRPA1) decreased, and this decrease was sharp for the NpHR opsin, and the chart of the TRPA1 opsin with a wavelength of 808 is lower than the others.

2. Materials and Methods

2.1. Basal Ganglia-Thalamic Network Model

Since Parkinson's disease affects the brain's basal ganglia, in this paper, a complete model including all the affected parts has been considered so that the study results are the closest to experimental and clinical studies, and we can study the influence of the performance of each part separately. For this purpose, the computational network model is based on the computational network model of Terman *et al.* [24, 25, 27, 29] and has been considered in such a way that it includes all the effective subsections of TH, GPi, GPe, and STN. MATLAB software has been used to establish BG-Th model and neural time series analysis. The numerical solution and discretization method have been applied to solve the equations to obtain and analyze the fire rate spectrums (see Appendix 1-9).

In Figure 1(a, b), the BG network model, which includes TH, GPi, GPe, and STN neurons and receives SMC input, has been shown along with sparse connections between TH, GPi, GPe, and STN cells in the BG network model. According to Figure 1a, STN provides excitatory input to GPe and GPi, GPe provides inhibitory input to STN, GPi, and GPe, and GPi also applies inhibitory input to TH.

By applying appropriate stimulation (three-mode and four-mode optogenetics for ChR2, NpHR, TRPV1, and TRPA1 opsins), the excitatory input from STN to GPi and the inhibitory input from GPe to GPi increases, followed by the inhibitory input from GPi to TH rises. In this mode, GPi increases the responsiveness of SMC by exerting inhibitory input to TH and improves TH function. In other words, GPi will be strong enough to improve TH performance. Otherwise, if proper stimulation is not applied, TH will respond to SMC input with an error. In Figure 1a, the yellow links show the three and four- states of optogenetic for different opsins of the ChR2, NpHR, TRPV1, and TRPA1 that have been applied to the GPe, GPi, and STN neurons.

SMC input has been considered a series of monophase current pulses with an amplitude of $3.5\ uA/cm^2 = 0.035pA/\mu m^2$ a pulse width of 5 ms. The I_{app} current is a constant and positive current to each GPi, GPe, and STN neuron. Also, ChR2 four-state optogenetic, NpHR three-state optogenetic, TRPV1 four-state optogenetic, and TRPA1 four-state optogenetic have been applied to STN, GPe, and GPi neurons. The neurons of the BG network model have been modeled as differential equations based on conductivity based on the Hodgkin-Huxley model. The membrane potential for TH, STN, GPe, and GPi neurons is calculated using Equations 1, 2, and 3, respectively. Numerical values of parameters and equations of the BG model have been selected from the reference [25].

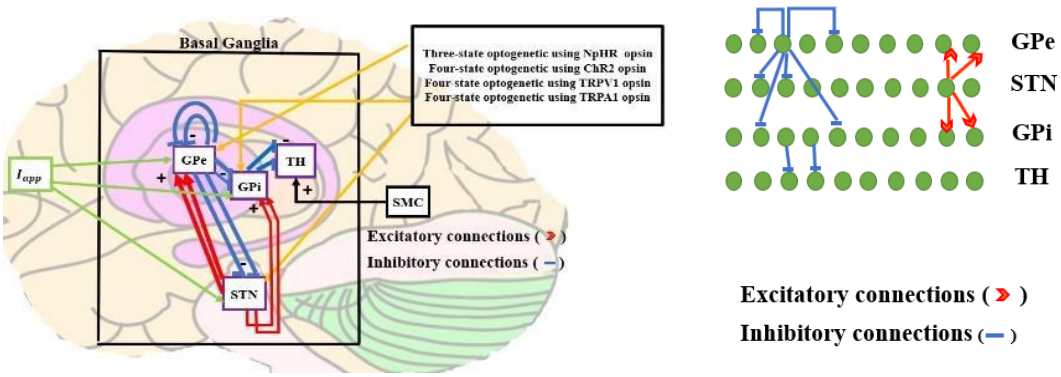

Figure 1. (a) BG network model consists of STN, GPe, GPi, and TH cells (b) Sparse connections between STN, GPe, GPi, and TH cells

$$C_m V' = -I_L - I_{Na} - I_K - I_T - I_{GPi\to Th} + I_{SMC} \quad (1)$$

$$C_m V' = -I_L - I_{Na} - I_K - I_T - I_{Ca} - I_{ahp} - I_{GPe\to STN} + I_{app} + I_{ChR2}(I_{NpHR}, I_{TRPV1}, I_{TRPA1}) \quad (2)$$

$$C_m V' = -I_L - I_{Na} - I_K - I_T - I_{Ca} - I_{ahp} - I_{STN\to GP} + I_{GPe\to GPe/GPi} + I_{app} + I_{ChR2}(I_{NpHR}, I_{TRPV1}, I_{TRPA1}) \quad (3)$$

Membrane currents include leak current (I_L), fast sodium and potassium currents (I_{Na},I_K), calcium currents (I_{Ca}, I_T), and voltage-independent K current activated by Ca (I_{ahp}), which are equal to (Equations 4-9):

$$\boldsymbol{I_L = g_L(v - E_L)} \quad (4)$$

$$\boldsymbol{I_{Na} = g_{Na} m_\infty(v)^3 h\,(v - E_{Na})} \quad (5)$$

$$\boldsymbol{I_K = g_K n^4\,(v - E_k)} \quad (6)$$

$$\boldsymbol{I_{Ca} = g_{Ca}\, s_\infty(v)^3 (v - E_{Ca})} \quad (7)$$

$$\boldsymbol{I_T = g_T a_\infty(v)^3 b_\infty(r)^2 r(v - E_T)} \quad (8)$$

$$\boldsymbol{I_{ahp} = g_{ahp}(v - E_{ahp})\left(\frac{CA}{CA + k_1}\right)} \quad (9)$$

Parameters $m_\infty, a_\infty, and\ s_\infty$ are immediate voltage-dependent gating variables, b_∞ which are sigmoidal functions of the time-dependent variable r. The intracellular Ca^{2+} concentration has been administered by calcium balance ($\frac{dCA}{dt} = \varepsilon(-I_{Ca} - I_T - k_{Ca} \times CA)$) . Gating variables of n, h, and r have been explained by $\frac{dx}{dt} = (x_\infty(V) - x)/\tau(V)$. The connection between network components (inhibitory and excitatory synapses) has been modeled by equation ($\frac{ds}{dt} = \alpha H_\infty(V_{presyn} - \theta_g)(1 - s) - \beta s$) for a segment of activated channels, where H_∞it is equal to $H_\infty(V) = 1/(1 + exp\,[-(V - \Theta_g^H)/\sigma_g^H]\,)$. Synaptic currents $I_{GPi\to Th}, I_{GPe\to STN}, I_{STN\to GP}, and\ I_{GPe\to GPe/GPi}$ have been defined as $I_{syn} = g_{syn}(V - V_{syn})\sum_j S_j$ [30]. The Hodgkin-Huxley model parameters, values, and units have been represented in Table 1 [31].

2.2. Sensory-Motor Cortex Input (SMC)

The sensory-motor cortex is a region of the brain that includes the precentral and postcentral gyri and includes the primary sensory and motor area of the brain, which was first introduced by Munk [32] in 1881. He called this part located in a large area in the visual and auditory centers of the brain, the sensory sphere. The sensory-motor cortex has neurons that play a role in controlling movement. The thalamus also consists of different nuclei, each of which plays a unique role, including receiving and transmitting sensory and motor signals in the form of impulses from the sensory-motor cortex [32]. Therefore, SMC is a signal input from the sensory-motor cortex to the thalamus [30]. In all references modeling brain neurons, it is considered as current pulses applied to TH neurons, as shown in Figure 1a. As in Equation 1, this signal input has been defined as I_{SMC} current and describes the sensory-motor cortex input to TH neurons. Therefore, I_{SMC} has been modeled as monophase pulses (in the form of a train of pulses) with Equation 10 [33] with the amplitude of $i_{SM} = 3.5uA/cm\text{^}2 = 0.035pA/\mu m^2$ and the pulse width of $\delta_{SM} = 0.3ms$ and the stimulation period of $\rho_{SM} = 7.7ms$ with Heaviside function of H to evoke an action potential with each pulse is applied to TH neurons.

$$I_{SM} = i_{SM} H\left(sin\ sin\left(\frac{2\pi t}{\rho_{SM}}\right)\right)[1 - H\left(sin\ sin\left(\frac{2\pi(t + \delta_{SM})}{\rho_{SM}}\right)\right) \quad (10)$$

2.3. Optogenetic Stimulation

In this section, we first introduced the models of four and three-state optogenetics. Then we described different light-sensitive and thermosensitive opsins, which are activated by visible light and NIR to inhibit or excite the activities of the neurons. In the four-state optogenetic model, a four-step transition is considered to receive light by opsin to follow the motion of the light stimulation. In this way, opsin molecules are initially in the closed state C. They transfer to the open state O_1 with light irradiation and to the open state O_2 with continued irradiation, and then they go to the C_2 state and return to the C_1 state when the light is turned

off. Meanwhile, in the three-state optogenetic model, opsin molecules are first in the closed state C, then go to the open state O when the light is exposed, then move to the dark state D and return to C when the light is turned off. According to the preliminary investigations and according to the information of the available reliable sources, considering that they have had closer results to the experimental conditions in the stimulation conditions considered, opsin of the NPHR as a three-state model and opsins of the ChR2, TRPV1, and TRPA1 have been simulated as a four-state model [21, 23, 31, 34-36]. So, in this study, we have chosen three and four-state optogenetic models for selected opsins.

2.3.1. Four-State Optogenetic Model

In this case, there is a four-state transition for the selective opsin, which is considered to follow the light-stimulated movement, Figurer 2a. Two open stages include O_1 and O_2, and two closed stages include C_1 and C_2. It should be noted that the open and closed stages are internal transition stages. The dynamics of transitions between stages are in the form of Equations 11, 12, 13, and 14 [24]:

$$\dot{O}_1 = \varepsilon_1 uF\,(1 - c_2 - o_1 - o_2) - (G_{d1} + e_{12})o_1 + e_{21}o_2 \quad (11)$$

$$\dot{O}_2 = \varepsilon_2 uFc_2 + e_{12}o_1 - (G_{d2} + e_{21})o_2 \quad (12)$$

$$\dot{C}_2 = G_{d2}o_2 - (P_2 u + G_r)c_2 \quad (13)$$

$$\dot{u} = (S_0(\emptyset) - u)/\tau_{opsin} \quad (14)$$

c_1, c_2, o_1 and o_2 show the fraction of selected opsin molecules in steps C_1, C_2, O_1, and O_2. ε_1, ε_2, G_{d1}, G_{d2}, e_{12}, e_{21}, and G_r are transmission rates. τ_{opsin} expresses the activity time of selective opsin ion and is equal to 1.5855 ms. For c_1, due to the existence of Equation 15, a relation has not been considered.

$$c_1 + c_2 + o_1 + o_2 = 1 \quad (15)$$

The selected opsin molecules are initially in the closed state C_1, then with light irradiation, they change to the open state O_1, and with continued radiation to the open state O_2, which has lower conductivity than O_1, or to C_1. After that, they either go to O_1 or C_2 again, and when the light turns off, they slowly return to the C_1 state [37]. The u function is related to the temporal movement of structural changes in proteins. The number of photons absorbed by selected opsin molecules per time unit equals $F = \sigma_{ret}\frac{\varphi}{w_{Loss}}$ [30]. Where σ_{ret}, the grid cross-section is equal to the value of $1.2 \times 10^{-20} m^2$. w_{Loss} is photons lost due to absorption and scattering. Photon transmission in each area is equal to $\varphi = \frac{\lambda A}{hc}$, where λ is the wavelength of the stimulation light used in nanometers, A is the intensity of the stimulation light, c is the speed of light, and h is Planck's constant [30]. The sigmoid function is in the form of Equation 16, in which $\emptyset(t)$ describes the stimulation steps in Equation 17.

$$S_0(\emptyset) = 0.5\,(1 + tanh\ tanh\ (120(\emptyset - 0.1))) \quad (16)$$

$$\emptyset(t) = \Theta\big(mod(t, P) - t_{off}\big) \quad (17)$$

Where Θ is the Heaviside function, P is the stimulation period, and t_{off} each cycle's time when there is no stimulation. Equation 18 defines the pulse width. Optical pulses are considered as Equation 19, A_{light} is the light intensity.

$$t_{on} = p - t_{off} \quad (18)$$

$$A(t) = A_{light}\emptyset(t) \quad (19)$$

The optical current of selective opsin is in the form of Equation 20. g_{opsin} is the maximum conductance of opsin in the O_1 stage and V_{Na} is the reversal potential of sodium, and γ is the conduction rate in the O_1 and O_2 stages [34]. The values of the four-state stimulation parameters have been represented in Table 1 [31].

$$I_{opsin} = g_{opsin}(V - V_{Na})(O_1 + \gamma O_2) \quad (20)$$

2.3.2. Three-State Optogenetic Model

The three-state model successfully predicts the peak and steady state of current and analyzes the movement of selective opsin. It provides a simple analysis mode that supports calculating deactivation and recovery time constants for optical currents. The three-state model includes open (O), closed (C), and dark stage (D), Figure 2b. Also, c, o, and d are a fraction of opsin. c is removed from the equation because the relation c+o+d=1 is established [34].

$$\dot{O} = \varepsilon F\emptyset(t)(1 - o - d) - G_d o \quad (21)$$

$$\dot{d} = G_d o - G_r d \quad (22)$$

$$F = \sigma_{ret} \frac{\varphi}{w_{Loss}} \quad (23)$$

$$\varphi = \frac{\lambda A}{hc} \quad (24)$$

$$A(t) = A_{light} \emptyset(t) \quad (25)$$

$$I_{opsin} = g_{opsin} VO \quad (26)$$

The number of photons absorbed by selected opsin molecules per unit of time is $F = \sigma_{ret} \frac{\varphi}{w_{Loss}}$ [30], where σ_{ret}, the grid cross-section, is equal to $1.2 \times 10^{-20} m^2$. w_{Loss} is photons lost due to absorption and scattering. The photon transmission in each area is equal to $\varphi = \frac{\lambda A}{hc}$. In which λ is the wavelength of light stimulation used in nanometers, A is the intensity of the light stimulation, c is the speed of light, and h is Planck's constant [30]. V is the membrane potential for opsin. The three-state stimulation parameter values have been represented in Table 1 [31].

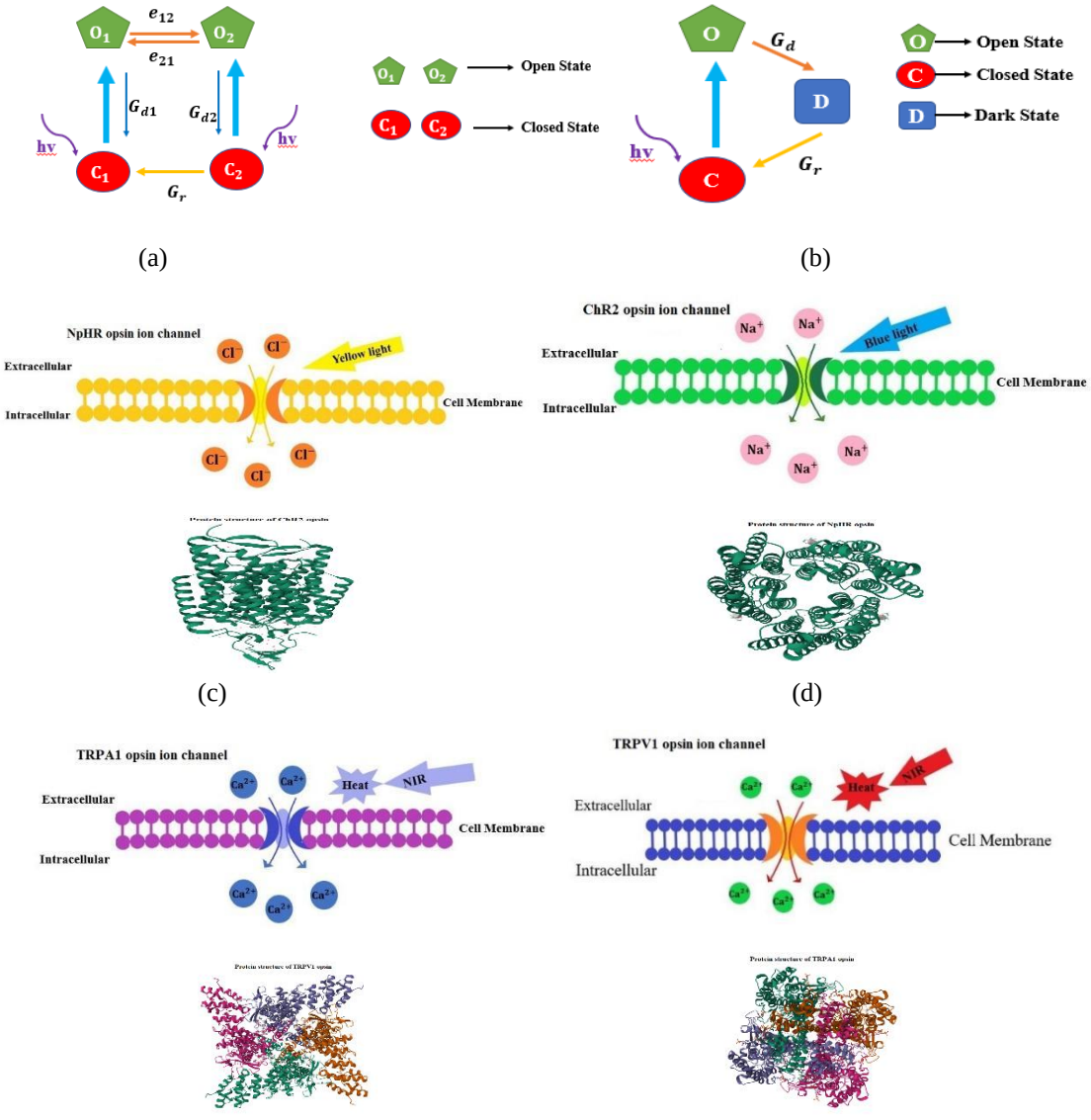

Figure 2. Photocycles of optogenetic stimulation, (a) four-state, (b) three -state. Opsins ion channels and protein structure of opsins, (c) ChR2, (d) NpHR, (e) TRPV1, (f) TRPA1

Table 1. Parameters values and descriptions for four and three-state Optogenetic and Hodgkin-Huxley model [31]

Parameter	Parameters description	Value and unit
	Transition rate of O_1 state	
	Transition rate of O_2 state	
	Transition rate for $O_1 \rightarrow C_1$	$\mathbf{4.6125\ ms^{-1}}$
ε_1		$\mathbf{2.1969\ ms^{-1}}$
ε_2	Transition rate for $O_2 \rightarrow C_2$	$\mathbf{0.1779\ ms^{-1}}$
G_{d1}		
G_{d2}	The recovery rate of C_1 after the light pulse	$\mathbf{0.2362\ ms^{-1}}$
G_r	turned off	$\mathbf{0.004\ ms^{-1}}$
e_{12}		$\mathbf{0.0696\ ms^{-1}}$
e_{21}	Transition rate for $O_1 \rightarrow O_2$	$\mathbf{0.0268\ ms^{-1}}$
ε		$\mathbf{0.4296\ ms^{-1}}$
G_r	Transition rate for $O_2 \rightarrow O_1$	$\mathbf{0.1385\ ms^{-1}}$
G_d	Transition tare for O state	$\mathbf{0.6518\ ms^{-1}}$
τ_{opsin}	Transition rate for $D \rightarrow C$	
σ_{ret}	Transition rate for $O \rightarrow D$	$\mathbf{1.5855\ m^2}$
h	Activation time of the opsin	1.2×10^{-20} m^2
c	Retinal cross-section	6.63×10^{-36} Js
λ	Planck's constant	3×10^8 m/s
g_{opsin}	Speed of light	480, 570, 808, 980 nm
	The wavelength of the light	$0.8755, \mathbf{2.4002}, \mathbf{10}, \mathbf{7.17\ nS/\mu m^2}$
	maximum conductance of opsin in O_1 state	
g_L of Th, STN, GP		
E_L of Th, STN, GP		
g_{Na} of Th, STN, GP	conductance of leak current	$\mathbf{0.05, 0.1, 2.25 nS/\mu m^2}$
	the voltage of the leak current	$\mathbf{-60, -65, -70}$ mv
E_{Na} of Th, STN, GP	conductance of fast sodium current	$\mathbf{37, 3, 120\ nS/\mu m^2}$
	the voltage of fast sodium current	$\mathbf{55, 50, 55\ mv}$
g_K of Th, STN, GP	conductance of fast potassium current	$\mathbf{45, 30, 30 nS/\mu m^2}$
	the voltage of fast potassium current	$\mathbf{-80, -75, -80\ mv}$
E_K of Th, STN, GP	conductance of calcium current	$\mathbf{5, 0.5, 0.5\ nS/\mu m^2}$
	the voltage of calcium current	$\mathbf{0\ mv}$
g_T of Th, STN, GP	conductance of calcium current	$\mathbf{2, 0.15\ nS/\mu m^2}$
	the voltage of calcium current	$\mathbf{140, 120\ mv}$
E_T of Th, STN, GP	conductance of voltage-independent K current	$\mathbf{20, 10\ nS/\mu m^2}$
	voltage of voltage-independent K current	$\mathbf{-80, -80\ mv}$
g_{Ca} of STN, GP		
E_{Ca} of STN, GP		
g_{ahp} of STN, GP		
E_{ahp} of STN, GP		

2.3.3. ChR2-Expression

In this paper, we have considered ChR2 as a light-sensitive opsin and applied it to the BG network model. ChR2 is a light-sensitive sodium channel for stimulating neurons by depolarizing neurons [27]; in Figure 2c, we have shown this ion channel in the neuron membrane and its protein structure. For this current to be comparable with previous theoretical studies and valid experiments, the current ChR2 (I_{ChR2}) in the form of pulses with a frequency of 100 Hz, pulse width of 5 ms, and a stimulation period of 10 ms with a number of 15 pulses (the same as in reference 35 used) [35]. I_{ChR2} is the current of the optogenetic stimulation called the photocurrent of the ChR2 opsin. I_{ChR2} can be defined by Equations 20 and 26.

2.3.4. NpHR-Expression

In this case, the NpHR opsin, the chlorine pump activated by yellow light with a wavelength of 570 nm,

has been chosen to stop neuronal activity with hyperpolarization [38]. The NpHR current (I_{NpHR}) is in the form of pulses with a frequency of 100 Hz, a pulse width of 5 ms, and a stimulation period of 10 ms with the number of 15 pulses (the same as in reference 31 used). In Figure 2d, the ion channel of NpHR opsin has been presented in the cell membrane and its protein structure [36].

2.3.5. Thermosensitive Ion Channels

To expand the use of optogenetic in clinical applications, it is necessary to develop optogenetic stimuli with high-conductivity opsins. The use of opsins or high conductivity leads to a decrease in the action of opsins on neurons, and temperature-sensitive opsins are one of these types of stimuli.

2.3.5.1. TRPV1-Expression

One of the most widely used temperature-sensitive opsins from the family of cationic TRP receptors is TRPV1, a type of calcium channel widely used in neurological disorders, especially in the brain. The current TRPV1 (I_{TRPV1}) is in the form of pulses with a frequency of 100 Hz, pulse width of 5 ms, and stimulation period of 10 ms with a number of 15 pulses. In Figure 2e, the ion channel of the opsin TRPV1 in the neuron membrane at a temperature higher than 43 degrees centigrade is opened, and its protein structure is also presented.

2.3.5.2. TRPA1-Expression

TRPA1 is one of the temperature-sensitive opsins from the family of cationic TRP receptors, a type of calcium channel widely used in neurological disorders, especially in the brain. TRPA1 has a high channel conductance (more than ChR2), making it an ideal target for developing chemo-optogenetic tools. The current TRPA1 (I_{TRPA1}) is in the form of pulses with a frequency of 100 Hz, pulse width of 5 ms, and stimulation period of 10 ms with a number of 15 pulses. In Figure 2f, the opsin TRPA1 ion channel in the neuron membrane that opens at temperatures below 30 and above 20 °C and its protein structure has been represented.

2.3.6. Evaluation of Network Performance

The performance of the BG network has been investigated by measuring how TH neurons respond to SMC input by considering EI. In other words, the EI is a method to quantify the function of the Th neurons by calculating the ratio of the error events to the SMC inputs. So, the EI of the BG network model appears to be an appropriate phenomenon for comparing stimulations. The EI described by Rubin and Treman [24] gives a quantitative measure of the accuracy of TH performance [25]. The network achieves optimal performance when each SMC input pulse generates an action potential in TH neurons. Three types of errors have been considered for TH neurons: spurious, burst, and miss events. The burst (^) exists when a neuron evokes more than one for one pulse of SMC input during 25 ms. The miss (*) occurs when one neuron can not evoke an action potential. The spurious happens when a TH cell evokes without stimulation. The EI is defined by Equation 27, where N_{miss} is the number of missed errors, N_{burst} is the number of burst errors, and N_{spur} is the number of spurious event errors of TH neurons in response to SMC input. The values of errors have been replaced from the firing rate graph of TH neurons, as shown in Figure 3a [34, 39]. Therefore, EI describes the value of the incorrect response to input pulses from the SMC compared to the total number of inputs of the SMC (N_{SM}, which we set in our simulations to be equal to 16 according to Fan *et al.* [40]), which indicates incorrect operation of the TH cells.

$$EI = \frac{N_{miss} + N_{burst} + N_{spur}}{N_{SM}} \quad (27)$$

On the other hand, two parameters of g_{syn} and I_{app} are changed by the dopamine disturbed in PD, where g_{syn} is the strength of synaptic connections between neurons, and I_{app} is the constant current applied to the model neurons from the striatum. Dopamine depletion leads to beta band oscillations and synchrony in the BG network model. Smaller values of I_{app} and large values of g_{syn} are associated with low levels of dopamine and high levels of beta band activity (excessive oscillation of BG neurons). The beta activity of the model has been defined as Equation 28 [34], where Var is the variance function, k is the scale factor, and is equal to 10^5. Beta activity has been depicted in Figure 3b, where the upper left corner has

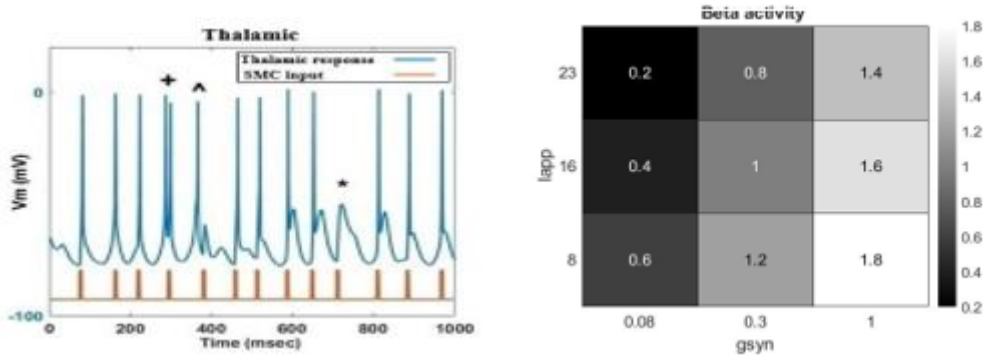

(a) (b)

Figure 3. (a) example of TH neurons response to SMC input, *: miss error, +: burst error, ^: spurious error, (b) Beta activity in the network by varying g_{syn} and I_{app}.

less beta activity, and the lower right corner has more beta activity. In general, lower levels of beta activity can be obtained with higher I_{app} and lower g_{syn}:

$$\beta_{act} = 1/n[Var(\sum_{i=1}^{n/2} S_{2i-1}) + Var(\sum_{i=1}^{\frac{n}{2}} S_{2i})]k \quad (28)$$

3. Results

As already mentioned, PD leads to disturbance in the function of BG network model neurons, so, the firing rate of STN, GPe, and GPi neurons changes and TH neurons respond to SMC input with errors. In this part, we have investigated the firing rate of neurons for both healthy and Parkinsonian states. When the STN, GPe, GPi, and TH cells are in a healthy and normal state, their firing rate is shown in Figure 4a. It can be seen that there is no error in TH neurons, and STN, GPe, and GPi neurons fire regularly and uniformly at fixed frequencies. The fire pattern of the Parkinsonian state is depicted in Figure 4b. The firing rate of STN and GPi cells has been increased and is not uniform, but the firing rate of GPe neurons has been decreased. The increase in the firing rate of GPi neurons in the Parkinsonian state causes TH cells to respond to the input stimulation pulses with more errors.

3.1. Results of Three-State Optogenetic Using NpHR Opsin and Four-State Optogenetic Using ChR2 Opsin

Since in PD mode, to improve the performance of the BG network model, it is necessary to apply appropriate stimulation to the neurons of the BG network model to examine the effects of three- and four-state optogenetic using NpHR and ChR2 opsins on EI, visible wavelength of 570 and 480 nm at frequencies of f=20-220 Hz with the number of pulses of ns=10-60 have been considered. The calculation results are represented in Figure 5. Examples of firing rates of STN, GPe, GPi, and TH in parkinsonian state with optogenetic application with opsin NpHR and wavelength of 570 nm for error-free state (f=140Hz, ns=50) in Figurer 5a, and for error state (f =60 Hz, ns=40) with two burst errors have been depicted in Figure 5b. Examples of firing rates of STN, GPe, GPi,

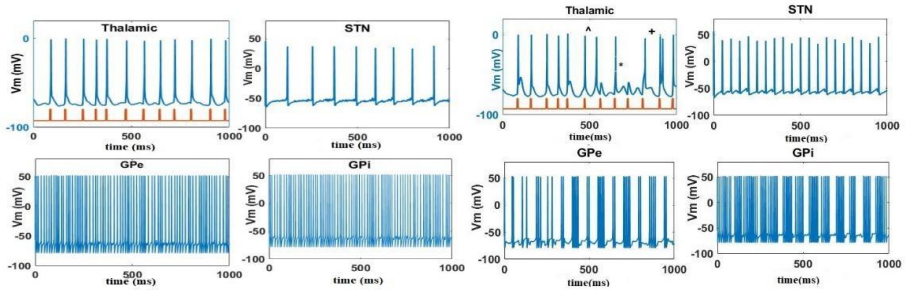

(a) (b)

Figure 4. Firing rates of STN, GPi, GPe, and TH cells for (a)Healthy state, (b) Parkinsonian state

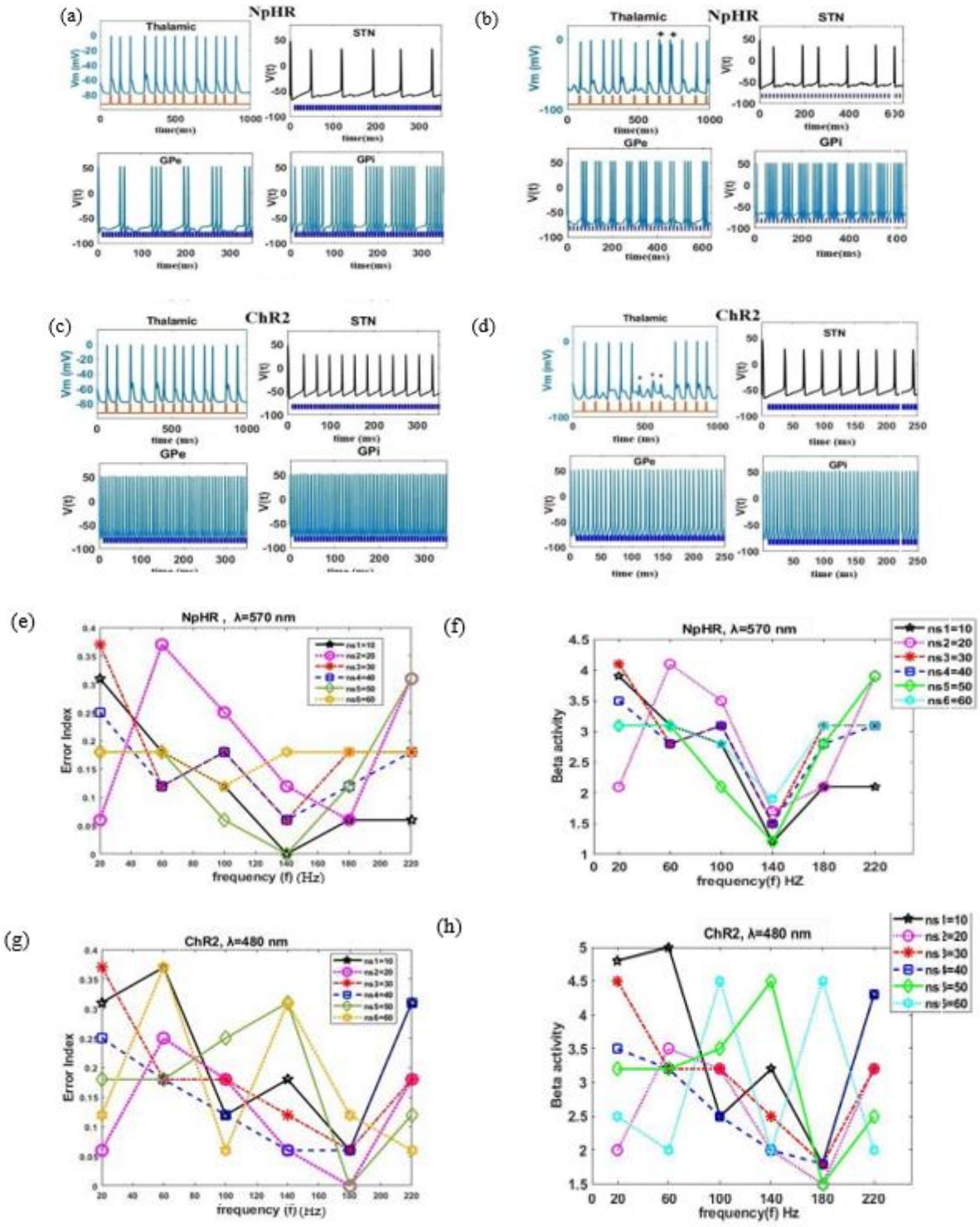

Figure 5. Firing rates of STN, GPe, GPi, TH for Parkinsonian state,(a) three-state optogenetic using NpHR opsin ($\lambda = 570nm$) and without error in f=140Hz, ns=50, (b) three-state optogenetic using NpHR opsin ($\lambda = 570nm$) with error in f=60Hz, ns=40, (c) four-state optogenetic using ChR2 opsin ($\lambda = 480nm$) without error in f=180 Hz, ns=50,(d)four-state optogenetic using ChR2 opsin ($\lambda = 480nm$) with errors in f=60 Hz, ns=40,(e) EI diagram for three-state NpHR ($\lambda = 570$ nm)for f=20-220 Hz and ns=10-60, (f) Beta activity for three-state NpHR(λ =570A nm) for f=20-220 Hz and ns=10-60,(g) EI diagram for four-state ChR2 ($\lambda = 480$ nm) for f=20-220 Hz and ns=10-60, (h) Beta activity for four-state ChR2(λ =480A nm) for f=20-220 Hz and ns=10-60

and TH cells without errors (f=180 Hz, ns=50) in Parkinsonian state with ChR2 for a visible wavelength of 480 nm have been shown in Figure 5c. The case with error (f=60Hz, ns=40) with three errors is

represented in Figure 5d. In addition, we have examined the EI plot and beta band for the frequencies (f=220-20 Hz) and the number of stimulation pulses (ns=10-60) with three-state optogenetic with NpHR opsin (570 nm visible light) and with four-state optogenetic with ChR2 opsin (480 nm visible light) and have brought its results in Figure 5 (e, f, g, h). According to the results of Figure 5e, f, in NpHR (570 nm) at the frequency of 140 Hz with 10 and 50 pulses, zero EI and beta band activity is at its lowest value (beta activity = 1.2) and in ChR2 (480 nm) at a frequency of 180 Hz with 20 and 50 pulses, EI is zero, and beta activity is minimal (beta activity = 1.5) (Figure 5g, h).

3.2. Results of Four-State Optogenetic Using TRPV1 Opsin

Since the use of NIR wavelength can lead to local heat and eventually cause damage to the brain tissue, temperature-sensitive opsins are needed to prevent damage to the brain tissue. For this purpose, four-state optogenetic effects using TRPV1 opsin on EI with NIR wavelengths of 808 and 980 nm at frequencies of f=20-220Hz and the number of pulses of ns=10-60 have been considered. The results of the calculations are shown in Figure 6. Examples of firing rates of STN, GPe, GPi, and TH neurons without errors in the Parkinsonian state with opsin TRPV1 for a wavelength of 808 nm and a frequency of 140 Hz and the number of stimulation pulses 40 in Figure 6a, and for a wavelength of 980 nm and the frequency of 20 Hz and the number of stimulation pulses of 30 have been shown in Figure 6b. For the Parkinsonian state with TPRV1 opsin with error, there are also examples of the firing rate of STN, GPe, and GPi cells at a wavelength of 808 nm and the frequency of 20 Hz and the number of stimulation pulses of 20 in Figure 6c, and at a wavelength of 980 nm and the frequency of 60 Hz with the number of stimulation pulses of 30 have been represented in Figure 6d.

As can be seen, there are two missing errors for 808 nm wavelength and two burst and spurious errors for 980 nm. We have presented the EI diagrams and beta band for the frequencies f=20-220 Hz and the number of stimulation pulses of ns=10-60 in wavelengths of 808 and 980 nm with four-state optogenetic TPRV1 in Figure 7. Based on the results at the wavelength of 808 nm for the frequency of 140 Hz with 30 and 40 pulses and the frequency of 180 with 30 pulses, EI is zero and its range of changes is from 0 to 0.4 (Figure 7a). The activity of the beta band is also for the frequency of 140 Hz With 30 and 40 pulses, the frequency of 180 Hz with 30 pulses, and the frequency of 20 Hz with 10 pulses is the lowest value (Beta activity = 0.2), and its variation range is 0 to 3.5 (Figure 7b). For the wavelength of 980 nm for the frequency of 20 Hz with 30 pulses and frequency of 100 with 20 pulses, EI is zero, and its range of changes is from 0 to 0.4 (Figure 7c). Beta band activity is also at the same frequencies, and the number of stimulation pulses has the lowest value (Beta activity =0.2). Its variation range is 0 to 4 (Figure 7d).

3.3. Results of Four-State Optogenetic Using TRPA1 Opsin

To further investigate the NIR wavelength (808 and 980 nm), we have considered another temperature-sensitive opsin called TRPA1 with four-state optogenetic at frequencies of f=20-220 Hz with the number of pulses of ns=10-60 and its results have been depicted in Figure 8. The firing rate of STN, GPe, GPi, and TH neurons without errors in the Parkinsonian state with TRPA1 for a wavelength of 808 nm and a frequency of 180 Hz and the number of stimulation pulses of 30 in Figure 8a, and for a wavelength of 980 nm and the frequency of 100 Hz and the number of stimulation pulses of 50 have been shown in Figure 8b. Also, examples of the firing rate of STN, GPe, GPi, and TH neurons for the Parkinsonian state, along with the error in the Parkinsonian state with opsin TRPA1 for a wavelength of 808 nm at a frequency of 100 Hz and the number of stimulation pulses 40 in Figure 8c, and for the wavelength 980 nm and frequency of 100 Hz and with 60 stimulation pulses have been presented in Figure 8d.

As can be seen, there are three missing errors for 808 nm wavelength and two burst errors for 980 nm. We have shown the plots of the EI and beta band activity for the frequencies of f=20-220 Hz and the stimulation pulses of ns = 10-60 at wavelengths of 808 and 980 nm with TRPA1 four-state optogenetic in Figure 9. According to the results for the wavelength of 808 nm, zero value for EI and the lowest value for beta band activity (Beta activity=0.2) is obtained at the frequency of 180 Hz with 30 pulses and at the frequency of 220 Hz with 50 pulses (Figure 9a, b). For

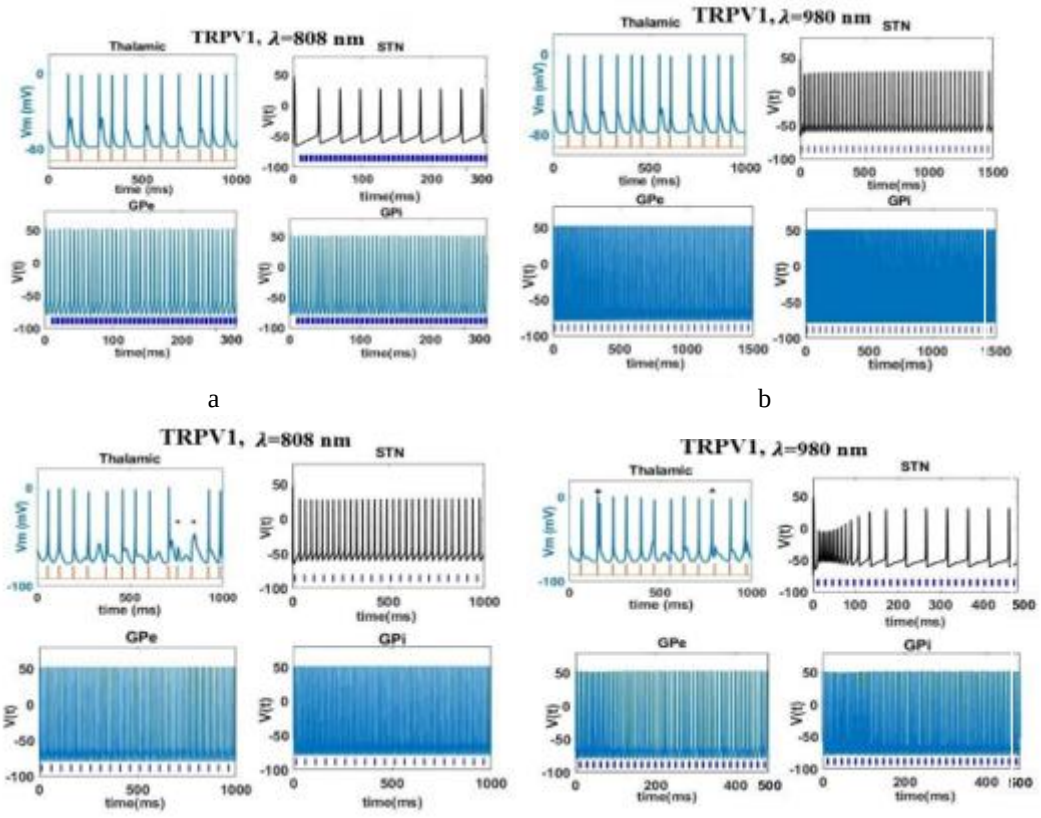

Figure 6. Firing rates of STN,GPe,GPi,TH for state with four-state optogenetic using TRPV1 opsin, (a) without error f=140Hz, ns=40.,λ=808 nm, (b) without error f=20Hz, ns=30,λ=980 nm, (c) with error f=20Hz, ns=20,λ=808 nm, (d) with error f=60Hz, ns=30,λ=980 nm

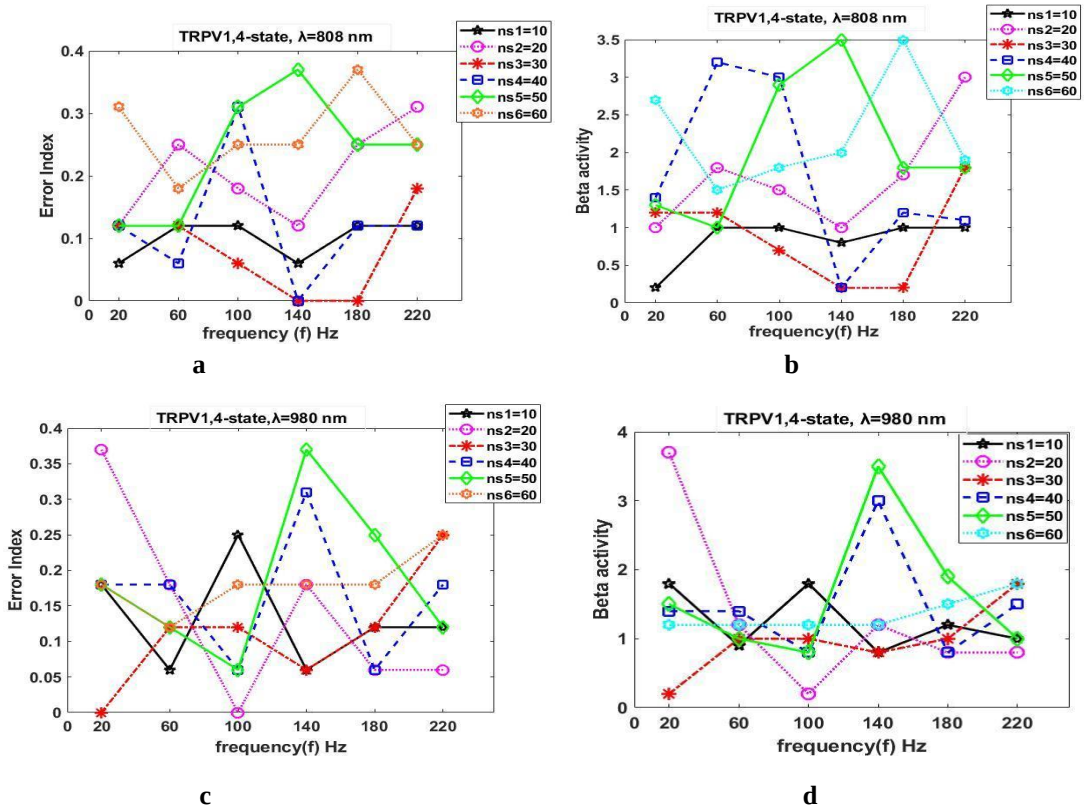

Figure 7. Four-state optogenetic using TPRV1 opsin for the frequencies of (f=20-220 Hz) and the number of stimulation pulses of (ns=10-60), (a) EI diagram for 808 nm, (b) Beta activity for 808 nm, (c) EI diagram for 980nm, (d) Beta activity for 980 nm

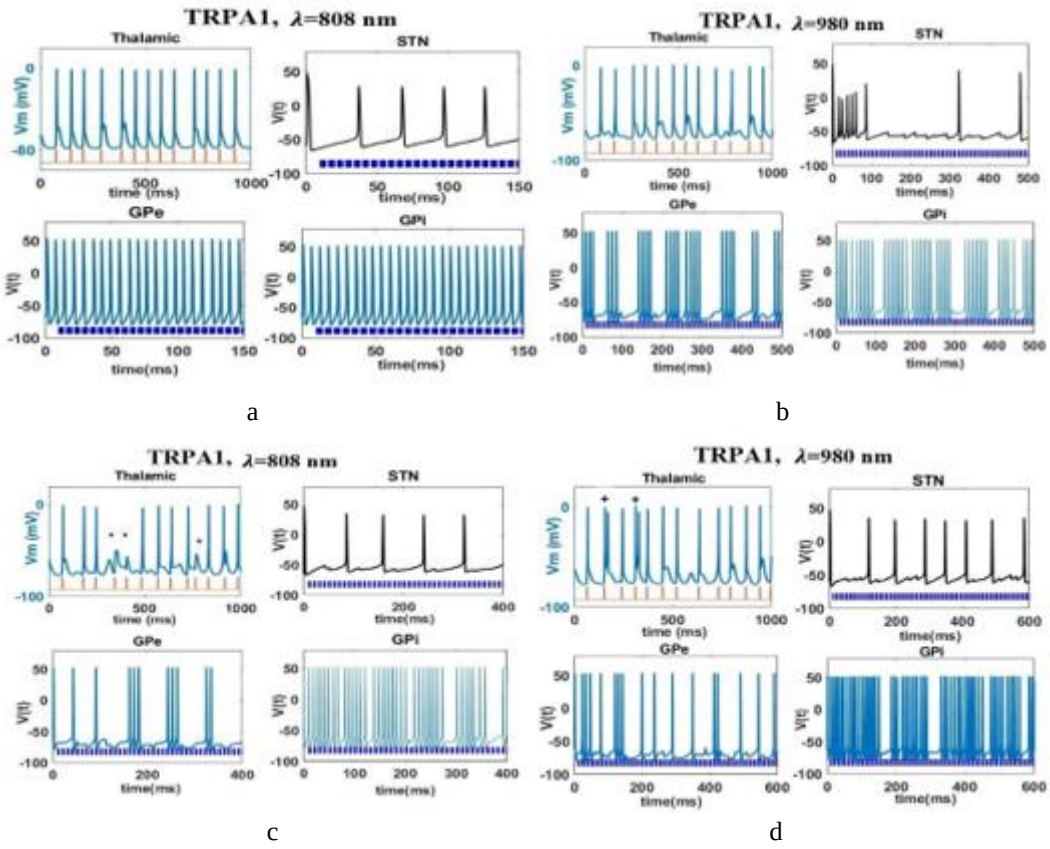

Figure 8. Firing rates of STN, GPe, GPi, and TH for Parkinsonian state with four-state optogenetic using TRPA1 opsin, (a) without error f=180Hz, ns=30,$\boldsymbol{\lambda = 808\ nm}$, (b) without error f=100Hz, ns=50,$\boldsymbol{\lambda = 980\ nm}$, (c) with error f=100Hz, ns=40,$\boldsymbol{\lambda = 808\ nm}$, (d) with error f=100Hz, ns=60,$\boldsymbol{\lambda = 980\ nm}$

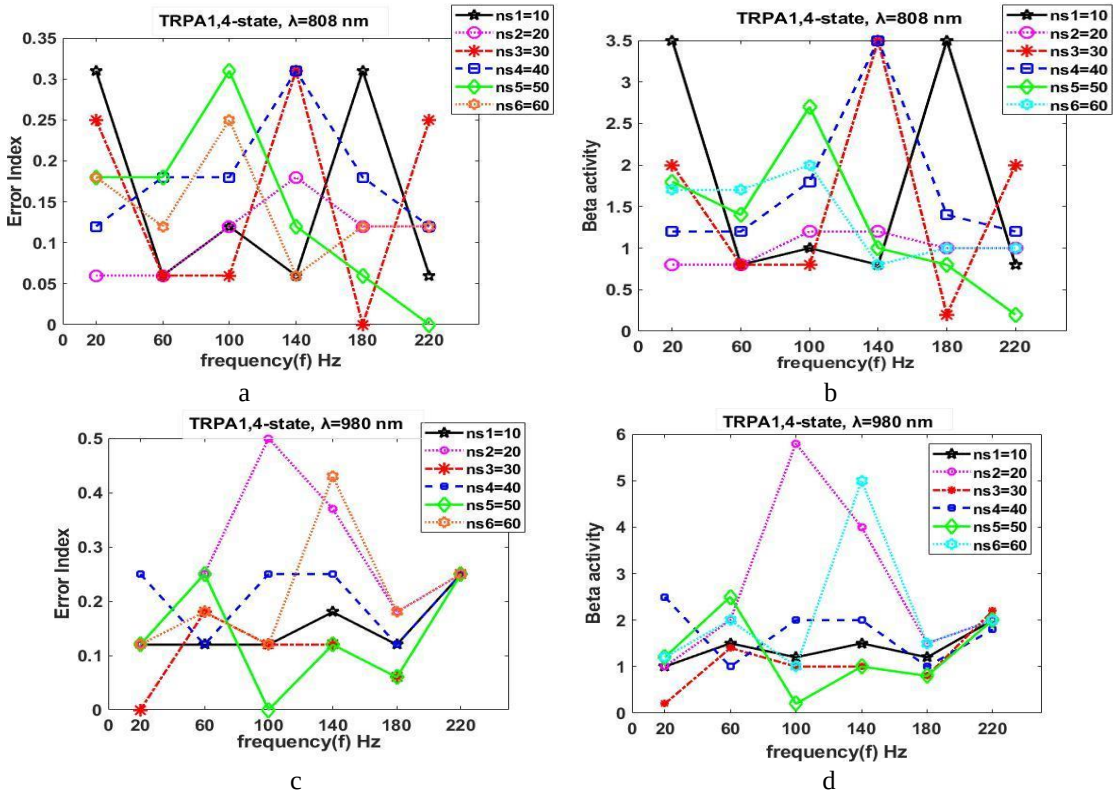

Figure 9. Four-state optogenetic using TPRA1 opsin for the frequencies of (f=20-220 Hz) and the number of stimulation pulses of (ns=10-60), (a) EI diagram for 808 nm, (b) Beta activity for 808 nm, (c) EI diagram for 980nm, (d) Beta activity for 980 nm

the wavelength of 980 nm at a frequency of 20 Hz with 30 pulses and a frequency of 100 Hz with 50 pulses, EI=0, and beta activity has the lowest value (Figure 9 c, d).

The range of changes for the wavelength of 808 nm for EI is from 0 to 0.35, and for the wavelength of 980 nm is from 0 to 0.5. Also, for the activity of the beta band, the range of changes for the wavelength of 808 nm is from 0 to 3.5, and for the wavelength of 980 nm is from 0 to 6.

We have compared our results with the results of experiments of two groups of monkeys shown in Figure 10 [25]. The effective range of EI for the first group of monkeys (Monkey R7160) is from 0 to 0.11, and for the second group of monkeys (Monkey R370) is from 0 to 0.03. For this purpose, EI bar graphs for opsins of NpHR (f=140Hz, λ=570nm), TRPV1(f=140Hz, λ=808nm), TRPV1(f=100Hz, λ=980nm), TRPA1(f=220Hz, λ=808nm), TRPA1(f=20Hz, λ=980nm) and ChR2 (f=180Hz, λ=480nm) for the number of stimulation pulses of ns=10-60 has been considered and the evaluation results have been represented in Figure 11. Based on the results, opsin of NpHR (f=140Hz, λ=570nm) in the number of pulses of 10 and 50 with both groups and in the number of pulses 30 and 40 with the first group, opsin of TRPV1(f=140Hz, λ=808nm) in the number of pulses of 30 and 40 with both groups and in the number of pulses of 10 with the first group, TRPV1 (f=100Hz, λ=980nm) in the number of pulses of 20 with both groups and in the number of pulses of 40 and 50 with the first group, TRPA1(f=220Hz,

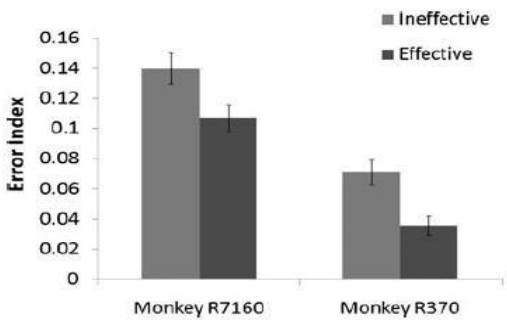

Figure 10. The results of experiments of two groups of monkeys [25]

λ=808nm) in the number of pulses of 50 with both groups of monkeys and in the number of pulses of with the first group, TRPA1 (f=20Hz, λ=980nm) in the number of pulses of 30 with both groups of monkeys and finally, ChR2 (f=180Hz, λ=480nm) corresponds to both groups in the number of pulses of 20 and 50 and to the first group in the number of pulses of 10, 30 and 40.

3.4. 3.4. Optimum Values of Parameters

In Table 2, the optimal values of frequency and number of stimulation pulses at EI are equal to zero and beta band activity at the lowest value for three-state optogenetic with NpHR opsin (570 nm), four-state optogenetic with opsin ChR2 (480 nm), four-state optogenetic with opsin TRPV1 (808 and 980 nm) and four-state optogenetic with opsin TRPA1 (808 and 980 nm) have been shown. In addition, by changing the intensity of the stimulation light (A_{light}) in the optimal frequency and number of stimulation pulses

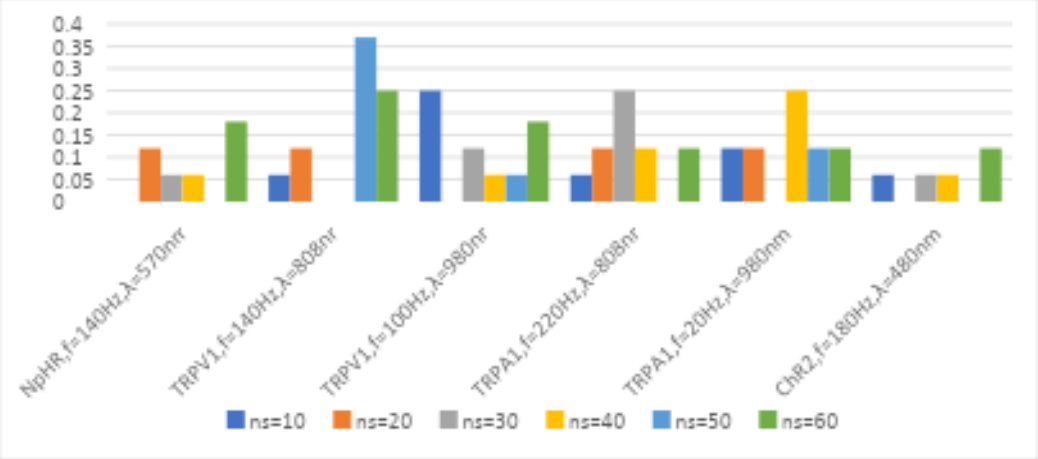

Figure 11. Diagrams of EI for the opsins of NpHR(f=140Hz, $\lambda = 570nm$,TRPV1(f=140Hz, $\lambda = 808nm$) ، TRPV1(f=100Hz, $\lambda = 980nm$),TRPA1(f=220Hz, $\lambda = 808nm$),TRPA1(f=20Hz, $\lambda = 980nm$)and ChR2(f=180Hz, $\lambda = 480nm$)

and visible and NIR wavelengths for each of three-state optogenetic stimulation with NpHR opsin, four-state optogenetic with ChR2 opsin, four-state optogenetic with TRPV1 opsin and TRPA1, we have investigated how the light intensity (A_{light}) affects the beta band activity and have shown the results in Figure 12.

Table 2. Optimal values of frequency, number of stimulation pulses in EI=0, and minimum beta activity for optogenetic opsins of NpHR($\lambda = 570nm$), ChR2($\lambda = 480nm$), TRPV1 ($\lambda = 808,980nm$), and TRPA1($\lambda = 808,980nm$)

Optogenetic Opsins	λ (nm)	f (Hz)	ns	Beta activity
NpHR, EI=0	570	140 140	10 50	1.2
ChR2 EI=0	480	180 180	20 50	1.5
TRPV1 EI=0	808	140 140 180	30 40 30	0.2
TRPV1 EI=0	980	20 100	30 20	0.2
TRPA1 EI=0	808	180 220	30 50	0.2
TRPA1 EI=0	980	20 100	30 50	0.2

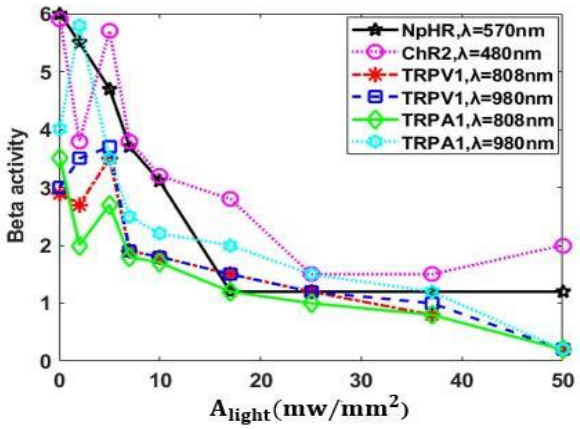

Figure 12. Diagrams of Beta activity and light intensity (A_{light}) in optimal parameters for, NpHR: $\lambda = 570\ nm$, f=140 Hz, ns=50, ChR2: $\lambda = 480\ nm$, f=180 Hz, ns=50,TRPV1: $\lambda = 808\ nm$, f=140 Hz, ns=40, TRPV1: $\lambda = 980\ nm$, f=100 Hz, ns=20, TRPA1: $\lambda = 808\ nm$, f=220 Hz, ns=50,TRPA1: $\lambda = 980\ nm$, f=20 Hz, ns=30

Based on the results of Figure 12, for NpHR opsin with a visible wavelength of 570 nm at the frequency of 140 Hz and 50 pulses, a sharp decrease in beta band activity can be seen with increasing A_{light} and from $A_{light} = 17mw/mm^2$ remains constant in the lowest value (1.2) for beta band activity. For opsin ChR2 with a visible wavelength of 480 nm at the frequency of 180 Hz and 50 pulses, with the increase of Alight, beta band activity is oscillatory then decreased, and from $A_{light} = 25mw/mm^2$ it is in the lowest value (1.5). For opsin TRPV1 with an NIR wavelength of 808 nm at the frequency of 140 Hz and 40 pulses, with increasing Alight, the beta band activity first decreased, then increased, and from $A_{light} = 7mw/mm^2$, the beta band activity decreased and the lowest value is equal to 0.2 in $A_{light} = 50mw/mm^2$.

For TRPV1 opsin with an NIR wavelength of 980 nm at the frequency of 100 Hz and 20 pulses, with the increase of Alight, the beta band activity increased, then decreased, and from $A_{light} = 7mw/mm^2$, the activity of the beta band decreased, and its lowest value is 0.2 in $A_{light} = 50mw/mm^2$. For opsin TRPA1 with an NIR wavelength of 808 nm at the frequency of 220 Hz and 50 pulses, with the increase of Alight, the activity of the beta band first decreased, then increased, and from $A_{light} = 7mw/mm^2$ in the activity of the band, a sharp decrease in the beta can be seen. Its lowest value equals 0.2 and is lower than the rest of the graphs. For opsin TRPA1 with an NIR wavelength of 980 nm at the frequency of 20 Hz and 30 pulses, with the increase of A_{light}, the activity of the beta band first increased, then decreased, and from $A_{light} = 10mw/mm^2$, the activity of the beta band decreased sharply, and its lowest value is 0.2.

4. Conclusion

Optogenetic stimulation is a powerful method to eliminate pathological symptoms caused by neurodegenerative diseases, especially Parkinson's disease. Optogenetic, by using light-sensitive ion channels (opsin/gene), stimulates or suppresses neuronal population activity. In this paper, we first applied the BG network model, including STN, GPe, GPi, and TH neurons, the three-state optogenetic with NpHR opsin and four-state optogenetic with ChR2 opsin, which are activated by visible light wavelengths of 570 and 480

nm, respectively, with the frequencies of f=20-220Hz and the number of pulses of ns=10-60 and we have studied its effects and obtained optimal values for frequency and number of pulses. Since the penetration depth of visible light in the brain tissue is low, it is necessary to implant an optical fiber in the brain tissue for the light delivery.

Therefore, we used the NIR wavelength, which has a significant penetration depth and is less invasive. Because NIR may damage the tissue by creating local heat, we have used temperature-sensitive opsins to prevent damage to the brain tissue. For this purpose, in the following, we have applied four-state optogenetic stimulation with TRPV1 and TRPA1 opsins with wavelengths of 808 and 980 nm with the frequencies of f=20-220Hz and number of stimulation pulses of ns=10-60 and have checked its effects on the firing rate of BG network model neurons and have obtained the optimal values for the basic parameters of the frequency and pulse number for each of the optogenetic stimulations and we have compared the results with the valid experimental results (two groups of monkeys).

Finally, by changing the intensity of light stimulation (Alight), we have obtained its effects on beta band activity for different three and four-state optogenetic stimulations for different opsins. So, the essential and basic parameters that influence the results include frequency (f), number of pulses (ns), and light stimulation intensity (Alight).

Based on the results, the optimal stimulation model is the four-state optogenetic stimulation with TRPA1 opsin at the wavelength of 808 nm with the best results and the smallest range for EI (from 0 to 0.35) and beta band activity (0 to 3.5). Four-state optogenetic stimulation with ChR2 opsin is more consistent with experimental results. Also, with the increase of Alight, the activity of the beta band for all opsins (NpHR, ChR2, TRPV1, and TRPA1) has decreased, and this decrease is sharp for NpHR opsin, and the graph of TRPA1 opsin with the wavelength of 808 is lower than the other graphs.

Identifying optimal conditions on the model of Parkinson's Disease BG-Th network model by inserting the four and three- states optogenetic stimulations with visible light and NIR by the effective light and thermal opsins of ChR2, NpHR, TRPV1, and TRPA1 causes to obtain the conditions in which the performance of the BG-Th network model has been improved and the PD pathological behavior disappeared. Therefore, in optimal conditions, the STN cells provide the excitatory input GPe cells supply appropriate inhibitory input to the GPi cells, and GPi cells can provide appropriate inhibitory input to the Th cells. As a result, its performance improves, and PD pathological behavior dissolves. So, by achieving the optimal conditions for the optogenetic stimulations, it is possible to achieve suitable ranges for essential and basic parameters such as frequency (f), number of stimulation pulses (ns), and light stimulation intensity (Alight) and introduce best conditions for clinical applications of optogenetic stimulation in PD is non-invasive or minimal invasive, the least damage to the brain tissue and provide the basis for influence clinical application of optogenetic stimulation in all kinds of neurodegenerative diseases, especially PD.

Appendix

```
function EI = BGnetwork(pd,wstim,freq)
%Usage: EI = BGnetwork(pd,wstim,freq)
%Example: error index=BG (1,1,130);
%Variables:
%pd - Variable to determine whether network is under the healthy or
%Parkinsonian condition. For healthy, pd = 0, for Parkinson's, pd = 1.
%wstim - Variable to determine wither deep brain stimulation is on.
%If DBS is off, wstim = 0. If DBS is on, wstim = 1.
%freq - Determines the frequency of stimulation, in Hz.
load('Istim.mat') %loads initial conditions
addpath('gating')
%%Membrane parameters
%In order of Th,STN,GP or Th,STN,GPe,GPi
Cm=1;
gl= [0.05 2.25 0.1]; El= [-70 -60 -65];
gnat= [3 37 120]; Ena= [50 55 55];
gk= [5 45 30]; Ek= [-75 -80 -80];
gt= [5 0.5 0.5]; Et=0;
gca= [0 2 0.15]; Eça= [0 140 120];
gahp= [0 20 10]; k1= [0 15 10]; kca= [0 22.5 15];
A= [0 3 2 2]; B= [0 0.1 0.04 0.04]; the= [0 30 20 20];
%%Synapse parameters
%In order of Igesn,Isnge,Igege,Isngi,Igigi,Igith
gsyn = [1 0.3 1 0.3 1 .08]; Esyn = [-85 0 -85 0 -85 -85];
tau=5; gpeak=0.43; gpeak1=0.3;
%time step
t=0: dt:tmax;
%%Setting initial matrices
vth=zeros(n,length(t)); %thalamic membrane voltage
vsn=zeros(n,length(t)); %STN membrane voltage
vge=zeros(n,length(t)); %GPe membrane voltage
vgi=zeros(n,length(t)); %GPi membrane voltage
S2=zeros(n,1); S21=zeros(n,1); S3=zeros(n,1);
S31=zeros(n,1); S32=zeros(n,1); S4=zeros(n,1);
Z2=zeros(n,1); Z4=zeros(n,1);
%%with or without dbs
Idbs=creatdbs(freq,tmax,dt); %creating DBS train with frequency freq
if ~wstim; Idbs=zeros (1, length(t)); end
%%initial conditions
vth (:1) =v1; vsn (:1) =v2; vge (:1) =v3; vgi (:1) =v4;
N2=stn_ninf (vsn (:1)); N3=gpe_ninf (vge (:1));
N4=gpe_ninf (vgi (:1)); H1=th_hinf (vth (:1));
```

```
H2=stn_hinf (vsn (:1)); H3=gpe_hinf(vge(:1));
H4=gpe_hinf(vgi(:1));R1=th_rinf(vth(:1));
R2=stn_rinf(vsn(:,1));R3=gpe_rinf(vge(:,1));
R4=gpe_rinf(vgi(:1));CA2=0.1;CA3=CA2;
 CA4=CA2; C2=stn_cinf (vsn(: ,1));
%%Time loop
for i=2: length(t)
V1=vth(:i-1);V2=vsn(:,i-1);V3=vge(:,i-1);  V4=vgi(:,i-1);
 % Synapse parameters
 S21(2: n) =S2(1: n-1); S21(1) =S2(n);
 S31(1: n-1) =S3(2: n); S31(n)=S3(1);
 S32(3: n) =S3(1: n-2); S32(1:2) =S3(n-1: n);
%membrane parameters
m1=th_minf(V1);          m2=stn_minf(V2);          m3=gpe_minf(V3);
m4=gpe_minf(V4);n2=stn_ninf(V2); n3=gpe_ninf(V3);
n4=gpe_ninf(V4);h1=th_hinf(V1);h2=stn_hinf(V2);
h3=gpe_hinf(V3);h4=gpe_hinf(V4); p1=th_pinf(V1);
a2=stn_ainf(V2);a3=gpe_ainf(V3);a4=gpe_ainf(V4);
b2=stn_binf(R2);s3=gpe_sinf(V3); s4=gpe_sinf(V4);
r1=th_rinf(V1);r2=stn_rinf(V2);r3=gpe_rinf(V3);
r4=gpe_rinf(V4);c2=stn_cinf(V2); tn2=stn_taun(V2);
tn3=gpe_taun(V3);tn4=gpe_taun(V4);th1=th_tauh(V1);th2=stn_tauh(
V2);th3=gpe_tauh(V3); th4=gpe_tauh(V4);
tr1=th_taur(V1);tr2=stn_taur(V2);tr3=30;tr4=30; tc2=stn_tauc(V2);
%thalamic cell currents
Il1=gl (1) *(V1-El (1));
Ina1=gna (1) *(m1. ^3). *H1. *(V1-Ena (1));
Ik1=gk (1) *((0.75*(1-H1)). ^4). *(V1-Ek (1));
It1=gt (1) *(p1. ^2). *R1. *(V1-Et);
Igith=1.4*gsyn (6) *(V1-Esyn (6)). *S4;
%STN cell currents
Il2=gl (2) *(V2-El (2));
Ik2=gk (2) *(N2. ^4). *(V2-Ek (2));
Ina2=gna (2) *(m2. ^3). *H2. *(V2-Ena (2));
It2=gt (2) *(a2. ^3). *(b2. ^2). *(V2-Eca (2));
Ica2=gca (2) *(C2. ^2). *(V2-Eca (2));
Iahp2=gahp (2) *(V2-Ek (2)). *(CA2. /(CA2+k1(2)));
Igesn=0.5*(gsyn(1)*(V2-Esyn(1)).*(S3+S31));          %Igesn=0;
Iappstn=33-pd*10;
%GPe cell currents
 Il3=gl (3) *(V3-El (3));
 Ik3=gk (3) *(N3. ^4). *(V3-Ek (3));
 Ina3=gna (3) *(m3. ^3). *H3. *(V3-Ena (3));
 It3=gt (3) *(a3. ^3). *R3. *(V3-Eca (3));
 Ica3=gca (3) *(s3. ^2). *(V3-Eca (3));
 Iahp3=gahp (3) *(V3-Ek (3)). *(CA3. /(CA3+k1(3)));
 Isnge=0.5*(gsyn(2) *(V3-Esyn(2)).*(S2+S21)); %Isnge=0;
 Igege=0.5*(gsyn(3)*(V3-Esyn(3)).*(S31+S32));          %Igege=0;
Iappgpe=21-13*pd+r;
 %GPi cell currents
 Il4=gl (3) *(V4-El (3));
 Ik4=gk (3) *(N4. ^4). *(V4-Ek (3));
 Ina4=gna (3) *(m4. ^3). *H4. *(V4-Ena (3));
 It4=gt (3) *(a4. ^3). *R4. *(V4-Eca (3));
 Ica4=gca (3) *(s4. ^2). *(V4-Eca (3));
 Iahp4=gahp (3) *(V4-Ek (3)). *(CA4. /(CA4+k1(3)));
 Isngi=0.5*(gsyn (4) *(V4-Esyn (4)). *(S2+S21)); %Isngi=0
 Igigi=0.5*(gsyn(5)*(V4-Esyn(5)).*(S31+S32));   %Igigi=0;%special
Iappgpi=22-pd*6;
%Differential Equations for cells
%thalamic
vth(:,i)=V1+dt*(1/Cm*(-Il1-Ik1-Ina1-It1 Igith+Istim(i)));
H1=H1+dt*((h1-H1)./th1); R1=R1+dt*((r1-R1)./tr1);
%STN
vsn(:i)=V2+dt*(1/Cm*(-Il2-Ik2-Ina2-It2-Ica2-Iahp2-
Igesn+Iappstn+Idbs(i)));
N2=N2+dt*(0.75*(n2-N2). /tn2);
H2=H2+dt*(0.75*(h2-H2). /th2);
R2=R2+dt*(0.2*(r2-R2). /tr2);
CA2=CA2+dt*(3.75*10^-5*(-Ica2-It2-kca (2) *CA2));
C2=C2+dt*(0.08*(c2-C2). /tc2);
a=find (vsn(: i-1)<-10 & vsn(:,i)>-10);
u=zeros(n,1); u(a)=gpeak/ (tau*exp (-1))/dt;
S2=S2+dt*Z2; zdot=u-2/tau*Z2-1/(tau^2) *S2;
Z2=Z2+dt*zdot;
%GPe
vge(: i)=V3+dt*(1/Cm*(-Il3-Ik3-Ina3-It3-Ica3-Iahp3-Isnge-
Igege+Iappgpe));
N3=N3+dt*(0.1*(n3-N3). /tn3);
H3=H3+dt*(0.05*(h3-H3). /th3);
R3=R3+dt*(1*(r3-R3). /tr3);
CA3=CA3+dt*(1*10^-4*(-Ica3-It3-kca (3) *CA3));
S3=S3+dt*(A (3) *(1-S3). *Hinf (V3-the (3))-B (3) *S3);
%GPi
vgi(:i)=V4+dt*(1/Cm*(-Il4-Ik4-Ina4-It4-Ica4-Iahp4-Isngi-
 Igigi+Iappgpi));
 N4=N4+dt*(0.1*(n4-N4). /tn4);
 H4=H4+dt*(0.05*(h4-H4). /th4);
 R4=R4+dt*(1*(r4-R4). /tr4);
 CA4=CA4+dt*(1*10^-4*(-Ica4-It4-kca (3) *CA4));
 a=find (vgi(: i-1)<-10 & vgi(:,i)>-10);
 u=zeros(n,1); u(a)=gpeak1/ (tau*exp (-1))/dt;
 S4=S4+dt*Z4; zdot=u-2/tau*Z4-1/(tau^2) *S4;
 Z4=Z4+dt*zdot;
 end
 %%Calculation of error index
 EI=calculateEI(t,vth,timespike,tmax);
 %%Plots membrane potential for one cell in each nucleus
  plotpotentials;
  return
```

2. CalculateEI

```
function er=calculateEI(t,vth,timespike,tmax)
%Calculates the Error Index (EI)
%Input:
%t - time vector (msec)
%vth - Array with membrane potentials of each thalamic cell
%timespike - Time of each SMC input pulse
%tmax - maximum time taken into consideration for calculation
%Output:
%er - Error index
m=size(vth,1); e=zeros (1, m);
b1=find(timespike>=200, 1); %ignore first 200msec
b2=find (timespike<=tmax-25, 1, 'last'); %ignore last 25 msec
for i=1:m
clear compare a b
compare= []; k=1;
for j=2: length (vth (i, :))
if vth(i, j-1)<-40 && vth(i,j)>-40
compare(k)=t(j); k=k+1;
end
end
for p=b1: b2
if p~=b2
a=find(compare>=timespike(p)&          ompare<timespike(p)+25);
b=find(compare>=timespike(p)+25 & compare<timespike(p+1));
elseif b2==length(timespike)
a=find(compare>=timespike(p) & compare<tmax);
b= []; else
a=find(compare>=timespike(p) & compare<timespike(p+1));
b=find(compare>=timespike(p)+25 & ompare<timespike(p+1)); end
if isempty(a)
e(i)=e(i)+1;
elseif size(a,2)>1
e(i)=e(i)+1;  end
if ~isempty(b)
e(i)=e(i)+length(b);     end   end   end
er=mean(e/(b2-b1+1));
```

```
return
```

3. Creatdbs

```
function ID=creatdbs(f,tmax,dt)
%Creates DBS train of frequency f, of length tmax (msec),
%with time step dt (msec)
t=0: dt:tmax; ID=zeros(1,length(t));iD=300;
pulse=iD*ones(1,0.3/dt); i=1; while i<length(t)
ID (i: i+0.3/dt-1) =pulse; instfreq=f; isi=1000/instfreq;
i=i+round(isi*1/dt);
end
```

4. CreateSMC

```
function [Istim, timespike]= createSMC(tmax,dt,freq,cv)
%creates Sensorimotor Cortex (SMC) input to thalamic cells
%Variables:
%tmax - length of input train (msec)
%dt - time step (msec)
%freq - frequency of input train
%cv - coefficient of variation of input train (gamma distribution)
%Output
%Istim - Input train from SMC
%timespike - Timing of each input pulse
t=0: dt:tmax;ism=3.5;Istim=zeros(1,length(t));deltasm=5;
pulse=ism*ones (1, deltasm/dt); i=1; j=1; A = 1/cv^2;
B = freq / A;if cv==0
instfreq=freq;else
 instfreq=gamrnd(A, B);
end
ipi=1000/instfreq;i=i+round(ipi/dt);
while i<length(t)timespike(j)=t(i);
Istim(i:i+deltasm/dt-1)=pulse;A = 1/cv^2;B  = freq / A;
if cv==0
instfreq=freq;else
instfreq=gamrnd(A, B);
end
ipi=1000/instfreq; i=i+round(ipi/dt);  j=j+1;
end
%ipi=timespike(2: end)-timespike(1:end-1);
return
```

5. Main_code

```
clear all
close all
%% Set initial conditions
%time variables
tmax=1000; %maximum time (ms)  dt=0.01; %timestep (ms)
t=0:dt:tmax;
n=10; %number of neurons in each nucleus (TH, STN, GPe, GPi)
%initial membrane voltages for all cells
v1=-62+randn(n,1)*5;v2=-62+randn(n,1)*5;
v3=-62+randn(n,1)*5;v4=-62+randn(n,1)*5;r=randn(n,1)*2;
%Sensorimotor cortex input to talamic cells
[Istim, timespike]=createSMC(tmax,dt,16,0.2);
%BGnetwork loads Istim.mat which has all the initial conditions
save('Istim.mat','Istim','timespike','tmax','dt','v1','v2','v3','v4','r','n');
%% Running BGnetwork.m
%For 1000msec with 10 neurons in each nucleus, each condition will
take
%roughly 60sec to run.
h=BGnetwork(0,0,0); %healthy
pd = BGnetwork(1,0,0); %PD
dbs=BGnetwork(1,1,130); %PD with Stimulation
```

6. Plotpotentials

```
figure; subplot (2,2,1);
ax=plotyy(t,vth(1,:),t,Istim(1:tmax/dt+1));
set (ax (1),'XLim', [0 tmax],'YLim', [-100 20],'Visible','on')
set (ax (2),'XLim', [0 tmax],'YLim', [-2 30],'Visible','off')
title('Thalamic'); ylabel('Vm (mV)'); xlabel('Time (msec)');
subplot (2,2,2); plot (t,vsn(1,:));axis([0 tmax -100 80 ])
title('STN'); ylabel('Vm (mV)'); xlabel('Time (msec)');
subplot (2,2,3); plot (t,vge(1,:));axis([0 tmax -100 80 ])
title('GPe'); ylabel('Vm (mV)'); xlabel('Time (msec)');
subplot (2,2,4); plot (t,vgi(1,:));axis([0 tmax -100 80 ])
title('GPi'); ylabel('Vm (mV)'); xlabel('Time (msec)');
```

7. Gating function of TH

```
function hinf=th_hinf(V); hinf=1. /(1+exp((V+41). /4)); return
function minf=th_minf(V); minf=1. / (1+exp (-(V+37). /7)); return
function pinf=th_pinf(V); pinf=1. / (1+exp (-(V+60). /6.2)); return
function rinf=th_rinf(V); rinf=1. /(1+exp((V+84). /4)); return
function tau=th_tauh(V); tau=1. /(ah(V)+bh(V));
function a=ah(V); a=0.128*exp (-(V+46). /18); function b=bh(V);
b=4. / (1+exp (-(V+23). /5)); return
function tau=th_taur(V); tau=0.15*(28+exp (-(V+25). /10.5)); return
function h=Hinf(V); h=1. / (1+exp (-(V+57). /2)); return
```

8. Gating function of STN

```
function ainf=stn_ainf(V); ainf=1. / (1+exp (-(V+63). /7.8)); return
function binf=stn_binf(R);
binf=1. / (1+exp (-(R-0.4). /0.1))-1/ (1+exp (0.4/0.1)); return
function cinf=stn_cinf(V); cinf=1. / (1+exp (-(V+20)/8)); return
function hinf=stn_hinf(V); hinf=1. /(1+exp((V+39). /3.1)); return
function hinf=stn_hinf(V); hinf=1. /(1+exp((V+39). /3.1)); return
function ninf=stn_ninf(V); ninf=1. / (1+exp (-(V+32). /8.0)); return
function rinf=stn_rinf(V); rinf=1. /(1+exp((V+67). /2)); return
function sinf=stn_sinf(V); sinf=1. / (1+exp (-(V+39). /8)); return
function tau=stn_tauc(V); tau=1+10. /(1+exp((V+80)/26)); return
function tau=stn_tauh(V); tau=1+500. / (1+exp (-(V+57). /-3)); return
function tau=stn_taun(V); tau=1+100. / (1+exp (-(V+80)./-26));return
function tau=stn_taun(V); tau=1+100. / (1+exp (-(V+80)./-26));return
function h=Hinf(V); h=1. / (1+exp (-(V+57). /2)); return
```

9. Gating function of GPe

```
function ainf=gpe_ainf(V); ainf=1. / (1+exp (-(V+57). /2)); return
function hinf=gpe_hinf(V); hinf=1. /(1+exp((V+58). /12)); return
function minf=gpe_minf(V); minf=1. / (1+exp (-(V+37). /10)); return
function ninf=gpe_ninf(V); ninf=1. / (1+exp (-(V+50). /14)); return
function rinf=gpe_rinf(V); rinf=1. /(1+exp((V+70). /2)); return
function sinf=gpe_sinf(V); sinf=1. / (1+exp (-(V+35). /2)); return
function tau=gpe_tauh(V); tau=0.05+0.27. / (1+exp (-(V+40). /-12)); return
function tau=gpe_taun(V); tau=0.05+0.27. / (1+exp (-(V+40). /-12)); return
function h=Hinf(V); h=1. / (1+exp (-(V+57). /2)); return
```

References

1- Ömer Faruk Ertuğrul, Yılmaz Kaya, Ramazan Tekin, and Mehmet Nuri Almalı, "Detection of Parkinson's disease by shifted one dimensional local binary patterns from gait." *Expert Systems with Applications*, Vol. 56pp. 156-63, (2016).

2- Marco Bisaglia, Roberta Filograna, Mariano Beltramini, and Luigi Bubacco, "Are dopamine derivatives implicated in the pathogenesis of Parkinson's disease?" *Ageing research reviews*, Vol. 13pp. 107-14, (2014).

3- Deepak Joshi, Aayushi Khajuria, and Pradeep Joshi, "An automatic non-invasive method for Parkinson's disease classification." *Computer methods and programs in biomedicine*, Vol. 145pp. 135-45, (2017).

4- Krystal L Parker, Youngcho Kim, Stephanie L Alberico, Eric B Emmons, and Nandakumar S Narayanan, "Optogenetic approaches to evaluate striatal function in animal models of Parkinson disease." *Dialogues in clinical neuroscience*, Vol. 18 (No. 1), pp. 99-107, (2016).

5- R Prashanth and Sumantra Dutta Roy, "Early detection of Parkinson's disease through patient questionnaire and

predictive modelling." *International journal of medical informatics*, Vol. 119pp. 75-87, (2018).

6- Rajamanickam Yuvaraj *et al.*, "Optimal set of EEG features for emotional state classification and trajectory visualization in Parkinson's disease." *International Journal of Psychophysiology*, Vol. 94 (No. 3), pp. 482-95, (2014).

7- Yuxia Liu, Zhigao Yi, Yun Yao, Bing Guo, and Xiaogang Liu, "Noninvasive manipulation of ion channels for neuromodulation and theranostics." *Accounts of Materials Research*, Vol. 3 (No. 2), pp. 247-58, (2022).

8- Bertil Hille, "Ion Channels of Excitable Membranes Third Edition." *(No Title)*, (2001).

9- Bing-Hong Lin, Ming-Shaung Ju, and Chou-Ching K Lin, "Suppression of acute and chronic mesial temporal epilepsy by contralateral sensing and closed-loop optogenetic stimulation with proportional-plus-off control." *Biomedical Signal Processing and Control*, Vol. 51pp. 309-17, (2019).

10- William L Hart, Karina Needham, Rachael T Richardson, Paul R Stoddart, and Tatiana Kameneva, "Dynamic optical clamp: a novel electrophysiology tool and a technique for closed-loop stimulation." *Biomedical Signal Processing and Control*, Vol. 85p. 105031, (2023).

11- Rahim Katyani and Shabnam Andalibi Miandoab, "Enhance efficiency in flat and nano roughness surface perovskite solar cells with the use of index near zero materials filter." *Optical and Quantum Electronics*, Vol. 53 (No. 9), p. 520, (2021).

12- James H Marshel *et al.*, "Cortical layer–specific critical dynamics triggering perception." *Science*, Vol. 365 (No. 6453), p. eaaw5202, (2019).

13- Seyed Hadi Badri, Mohsen Mohammadzadeh Gilarlue, Hadi Soofi, and Hassan Rasooli Saghai, "3× 3 slot waveguide crossing based on Maxwell's fisheye lens." *Optical Engineering*, Vol. 58 (No. 9), pp. 097102-02, (2019).

14- Lief Fenno, Ofer Yizhar, and Karl Deisseroth, "The development and application of optogenetics." *Annual review of neuroscience*, Vol. 34 (No. 1), pp. 389-412, (2011).

15- Panpan Rao *et al.*, "Near-infrared light driven tissue-penetrating cardiac optogenetics via upconversion nanoparticles in vivo." *Biomedical Optics Express*, Vol. 11 (No. 3), pp. 1401-16, (2020).

16- Ye-Fu Wang, Gao-Yuan Liu, Ling-Dong Sun, Jia-Wen Xiao, Jia-Cai Zhou, and Chun-Hua Yan, "Nd3+-sensitized upconversion nanophosphors: efficient in vivo bioimaging probes with minimized heating effect." *ACS nano*, Vol. 7 (No. 8), pp. 7200-06, (2013).

17- Sounderya Nagarajan and Yong Zhang, "Upconversion fluorescent nanoparticles as a potential tool for in-depth imaging." *Nanotechnology*, Vol. 22 (No. 39), p. 395101, (2011).

18- Eugene Gussakovsky and Valery Kupriyanov, "Assessment of near-infrared path length in fibrous phantom and muscle tissue." *Applied spectroscopy*, Vol. 62 (No. 6), pp. 671-76, (2008).

19- Elham Amini *et al.*, "Solution-processed photoconductive UV detectors based on ZnO nanosheets." *IEEE Photonics Technology Letters*, Vol. 24 (No. 22), pp. 1995-97, (2012).

20- Esmaeil Parcham and Shabnam Andalibi Miandoab, "Introducing nanostructure patterns for performance enhancement in PbS colloidal quantum dot solar cells." *International Journal of Nano Dimension*, Vol. 11 (No. 1), pp. 18-25, (2020).

21- Wei-Hsu Chen, Taiki Onoe, and Masao Kamimura, "Noninvasive near-infrared light triggers the remote activation of thermo-responsive TRPV1 channels in neurons based on biodegradable/photothermal polymer micelles." *Nanoscale*, Vol. 14 (No. 6), pp. 2210-20, (2022).

22- Raquibul Hasan and Xuming Zhang, "Ca2+ regulation of TRP ion channels." *International journal of molecular sciences*, Vol. 19 (No. 4), p. 1256, (2018).

23- Pui-Ying Lam *et al.*, "TRPswitch—A step-function chemo-optogenetic ligand for the vertebrate TRPA1 channel." *Journal of the American Chemical Society*, Vol. 142 (No. 41), pp. 17457-68, (2020).

24- Jonathan E Rubin and David Terman, "High frequency stimulation of the subthalamic nucleus eliminates pathological thalamic rhythmicity in a computational model." *Journal of computational neuroscience*, Vol. 16pp. 211-35, (2004).

25- Rosa Q So, Alexander R Kent, and Warren M Grill, "Relative contributions of local cell and passing fiber activation and silencing to changes in thalamic fidelity during deep brain stimulation and lesioning: a computational modeling study." *Journal of computational neuroscience*, Vol. 32 (No. 3), pp. 499-519, (2012).

26- Choongseok Park, Robert M Worth, and Leonid L Rubchinsky, "Neural dynamics in Parkinsonian brain." *Physical Review E-Statistical, Nonlinear, and Soft Matter Physics*, Vol. 83 (No. 4), (2011).

27- Honghui Zhang, Ying Yu, Zichen Deng, and Qingyun Wang, "Activity pattern analysis of the subthalamopallidal network under ChannelRhodopsin-2 and Halorhodopsin photocurrent control." *Chaos, Solitons & Fractals*, Vol. 138p. 109963, (2020).

28- SV Gudkov *et al.*, "Effect of visible light on biological objects: Physiological and pathophysiological aspects." *Physics of Wave Phenomena*, Vol. 25pp. 207-13, (2017).

29- David Terman, Jonathan E Rubin, AC Yew, and CJ Wilson, "Activity patterns in a model for the subthalamopallidal network of the basal ganglia." *Journal of Neuroscience*, Vol. 22 (No. 7), pp. 2963-76, (2002).

30- Roxana A Stefanescu, RG Shivakeshavan, Pramod P Khargonekar, and Sachin S Talathi, "Computational modeling of channelrhodopsin-2 photocurrent characteristics in relation to neural signaling." *Bulletin of mathematical biology,* Vol. 75pp. 2208-40, (2013).

31- Nazlar Ghasemzadeh, Fereidoun Nowshiravan Rahatabad, Siamak Haghipour, Shabnam Andalibi Miandoab, and Keivan Maghooli, "Controlling pathological activity of Parkinson basal ganglia based on excitation and inhibition optogenetic models and monophasic and biphasic electrical stimulations." *Journal of Biosciences,* Vol. 48 (No. 4), p. 40, (2023).

32- ALFRED Meyer, "The concept of a sensorimotor cortex: its early history, with especial emphasis on two early experimental contributions by W. Bechterew." *Brain: a journal of neurology,* Vol. 101 (No. 4), pp. 673-85, (1978).

33- Jessica A Cardin *et al.*, "Targeted optogenetic stimulation and recording of neurons in vivo using cell-type-specific expression of Channelrhodopsin-2." *Nature protocols,* Vol. 5 (No. 2), pp. 247-54, (2010).

34- Shivakeshavan Ratnadurai-Giridharan, Chung C Cheung, and Leonid L Rubchinsky, "Effects of electrical and optogenetic deep brain stimulation on synchronized oscillatory activity in parkinsonian basal ganglia." *IEEE Transactions on Neural Systems and Rehabilitation Engineering,* Vol. 25 (No. 11), pp. 2188-95, (2017).

35- Nazlar Ghasemzadeh, Fereidoun Nowshiravan Rahatabad, Siamak Haghipour, Shabnam Andalibi Miandoab, and Keivan Maghooli, "Effect of Optogenetic Stimulation Parameters on Firing Rate of Basal Ganglia Neurons in Parkinsonian State BG and RT Networks." *Frontiers in Biomedical Technologies,* (2024).

36- Nazlar Ghasemzadeh, Fereidoun Nowshiravan Rahatabad, Siamak Haghipour, Shabnam Andalibi Miandoab, and Keivan Maghooli, "Controlling the pathological activity of parkinsonian basal nuclei with the basal ganglia network model under light stimulation in the three-state, four-state channelrhodopsin, and three-state halorhodopsin optogenetic models." *Medical Journal of Tabriz University of Medical Sciences,* Vol. 46 (No. 3), pp. 275-93, (2024).

37- Zahra Noraepour, Mohammad Ismail Zibaii, Leila Dargahi, and hamid Latifi, "Modeling and study of Rhodopsin proteins responses to laser light irradiance in ultrafast optogenetic control." (in eng), *Accepted and Presented Articles of OPSI Conferences,* Research Vol. 24 (No. 0), pp. 569-72, (2018).

38- Viviana Gradinaru, Kimberly R Thompson, and Karl Deisseroth, "eNpHR: a Natronomonas halorhodopsin enhanced for optogenetic applications." *Brain cell biology,* Vol. 36pp. 129-39, (2008).

39- André Berndt *et al.*, "High-efficiency channelrhodopsins for fast neuronal stimulation at low light levels." *Proceedings of the National Academy of Sciences,* Vol. 108 (No. 18), pp. 7595-600, (2011).

40- Denggui Fan, Zhihui Wang, and Qingyun Wang, "Optimal control of directional deep brain stimulation in the parkinsonian neuronal network." *Communications in Nonlinear Science and Numerical Simulation,* Vol. 36pp. 219-37, (2016).